Development of Low Loss Active Magnetic Bearing for the Flywheel UPS *

Gen Kuwata, Noriyasu Sugitani, and Osamu Saito
Machine Element Dept. Research Laboratory
Ishikawajima-Harima Heavy Industries Co., Ltd.
Yokohama, Kanagawa-Pref., 235-8501, Japan
gen_kuwata@ihi.co.jp

***Abstract* – The flywheel for the uninterruptive power supply (UPS) is required to be lower mechanical loss during high-speed rotation. We developed low loss active magnetic bearing (AMB), and applied it to the prototype of the flywheel UPS. As a result, the AMB could support up to rated rotational speed at maximum load, and measured mechanical loss was very low. In this paper, we mentioned the design, analysis and the results of rotating test.**

***Index Terms* – Flywheel, Magnetic Bearing, UPS, Zeropower Control, Low Loss**

I. Introduction

The UPS is a device to protect such network equipments as computers, servers and large-scale data centres from the power failure. The lead battery type and the capacitor type are mainly used, however the flywheel UPS is highlighted recently. Because cost of the flywheel UPS is cheaper, size is smaller, life is longer and it is friendlier to environment compared with the other types. To store the electric power as rotating energy, mechanical loss must be kept at the very low level. In the past, we had developed 10kW-h flywheel energy storage system [1] and very low loss AMB. Now, we are developing low energy loss AMB for the flywheel UPS. The present paper shows the design and test results of the flywheel UPS using AMB.

II. Specification for System

The specification for the flywheel UPS is shown in TABLE I. The rotor is composed of a main shaft, an induction motor/generator, a CFRP flywheel, an aluminum hub which connects the CFRP flywheel and main shaft. The whole system is enclosed in the vacuum chamber for reducing windage loss during high-speed rotation as low as possible.

III. Design and Analysis

A. Design of Rotor and AMB

At first, the moment of inertia of the rotor, the rotor configuration and the rated rotational speed were decided as generating electric power for 20seconds at 200kW.

* This work is partially supported by Japanese public agency, New Energy and Industrial Technology Development Organization (NEDO).

The rotor is supported by radial AMBs and thrust AMB. This system of rotor and AMB is shown in Fig.1, and the photograph of rotor is shown in Fig.2. Auxiliary bearings composed of ceramic balls and stainless steal are set upper and lower of the rotor. The rated rotational speed was determined to operate under bending critical speed.

In order to make loss lower, radial AMBs were designed as follows.

1) The homo-polar type was applied, because it was able to make loss lower than the hetero-polar type.

2) The electromagnets were miniaturized and multipolarized to decrease the iron loss in the core. Concretely, one actuator is divided two electromagnets in the direction of the circumference, and the coils of two electromagnets are connected with series.

TABLE I
Characteristics of Flywheel UPS

Energy Storage	1.7kW-h
Motor/Generator Type	Induction Type
Motor/Generator Power	200kW
Compensating Time	20s
Rated Rotational Speed	13,000min^{-1}
Rotor Mass	254kg
Flywheel Material	Carbon Fiber Reinforced Plastic (CFRP)
Flywheel Diameter	700mm
Flywheel Tip Speed	476m/s
Pressure in the Chamber	Less than 0.1Pa

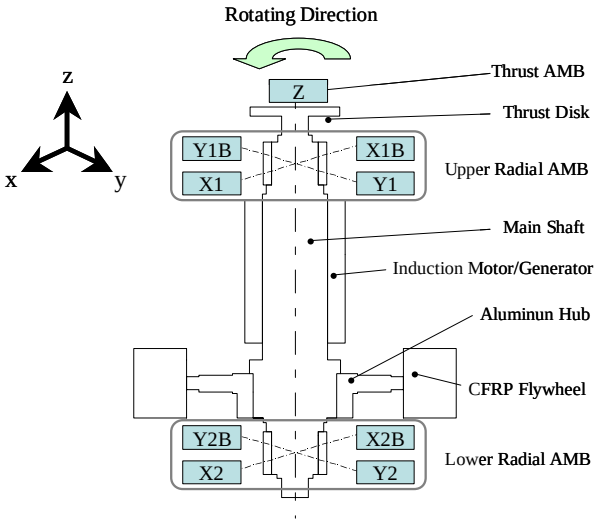

Fig.1 Structure of Rotor and AMB System

From above-mentioned, it is expected to be able to control AMB up to high frequency because the coil inductance decrease in the high frequency region is suppressed.

3) The nonlinear zeropower method [2] proposed by Nonami et al. was adopted for AMB control. It is able to reduce the eddy current loss, because it does not use the bias current.

4) The smaller tip speed is, the more the eddy current loss can be reduced. Therefore, the journal diameter was decided so that the journal tip speed might be less than 100m/s. The details of the radial AMBs are shown in TABLE II.

B. Analysis Model

The rotor system was modelled as three shafts which were connected by using spring elements, and the natural frequencies of the rotor were calculated by the transfer matrix method. The analysis model is shown in Fig.3.

As a result, there were two rigid modes and three bending modes, one of which was bending mode of flywheel hub and the other two were bending mode of the rotor. Fig.4 shows the mode shape in each natural frequency. In addition, to grasp a detailed mode shape of bending mode of flywheel hub shown in Fig.4(b), it was analysed by FEM. Fig.5 shows a hub bending mode at 0min^{-1} obtained by FEM analysis.

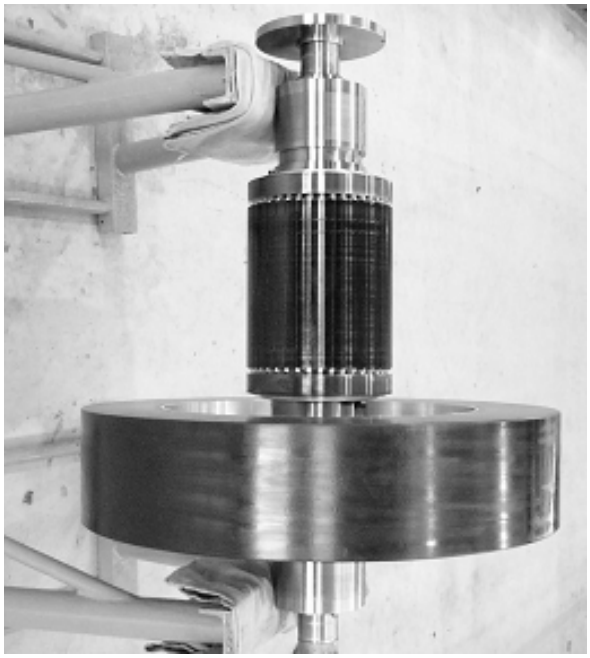

Fig.2 Photograph of Rotor

TABLE II
PARAMETERS OF THE ROTOR AND RADIAL AMB SYSTEM

Journal Diameter	140mm
Journal Tip Speed	95m/s
Area of Electromagnet	Total 1064mm2
Coil Turn	Total 200Turn (100Turn / 1Electromagnet)
Air Gap at Equilibrium State	0.45mm
Touchdown Gap	0.2mm
Inductance	28mH

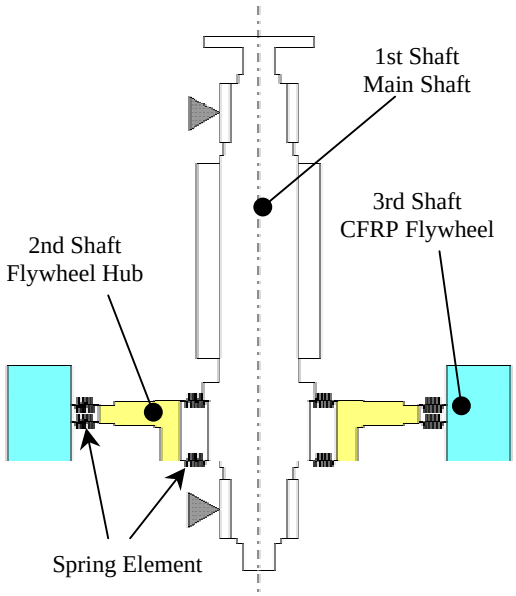

Fig.3 Analysis Model of Rotor Dynamics

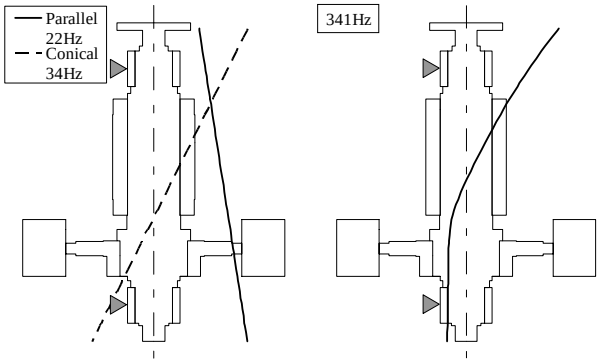

(a) Two Rigid Modes (b) Bending Mode of Flywheel Hub

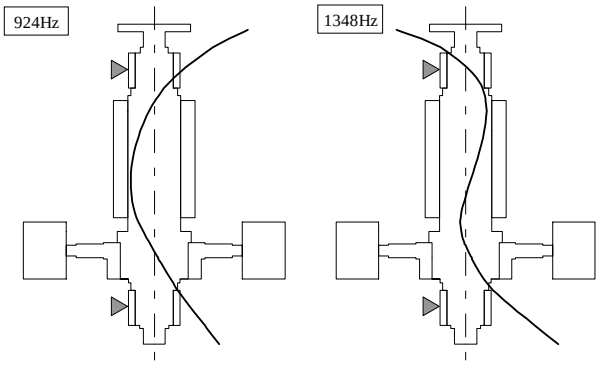

(c) 1st Rotor Bending Mode (d) 2nd Rotor Bending Mode

Fig.4 Mode Shape at 0min^{-1}

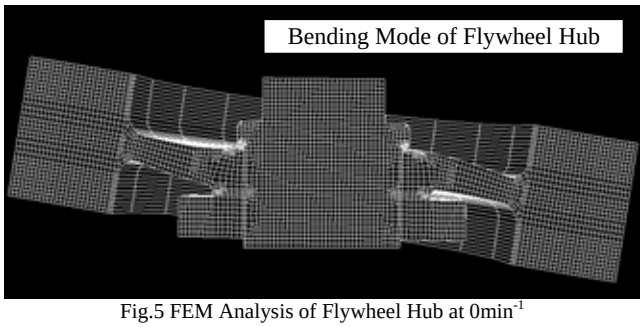

Fig.5 FEM Analysis of Flywheel Hub at 0min^{-1}

C. AMB Controller

The model of X1-axis is shown in Fig.6. In X1-Axis, two electromagnets are set at the opposite side, and radial AMB is controlled side by side. The equation of motion is as follows.

$$m\ddot{x} = k_m \left\{ i_{x1}^2 / (X_0 - x)^2 - i_{x1B}^2 / (X_0 + x)^2 \right\} \quad (1)$$

$$k_m = \mu_0 N^2 S / 4 \quad (2)$$

X_0 : Air gap at equilibrium state (m)
x : Rotor displacement from equilibrium state (m)
i_{x1}, i_{x1B} : Coil current of X1, X1B (A)
m : Mass (kg)
k_m : Constant of magnetic attractive force (Nm^2/A^2)
μ_0 : Permeability in the vacuum (H/m)
N : Coil turn (-)
S : Area of electromagnet per a pole (m^2)

Normally, a bias current is used for linear approximation around equilibrium point. In case of zeropower method, a control current is supplied to one of the coils of electromagnets and it is controlled in nonlinear region. Substituting the coil current based on nonlinear zeropower method into (1), (1) is expressed by using a (>1), γ (>0) as follows.

$$\ddot{x} = -2a^2 x - 2a^2 \gamma \dot{x} \quad (3)$$

Equation (3) is equivalent to the equation of one degree of freedom system with damping. Natural angular frequency ω_n and damping ratio ς can be determined arbitrarily according to (4), (5), and zeropower method can generate positive stiffness and positive damping for two rigid modes in this way.

$$\omega_n = \sqrt{2}a \quad (4)$$

$$\varsigma = a\gamma / \sqrt{2} \quad (5)$$

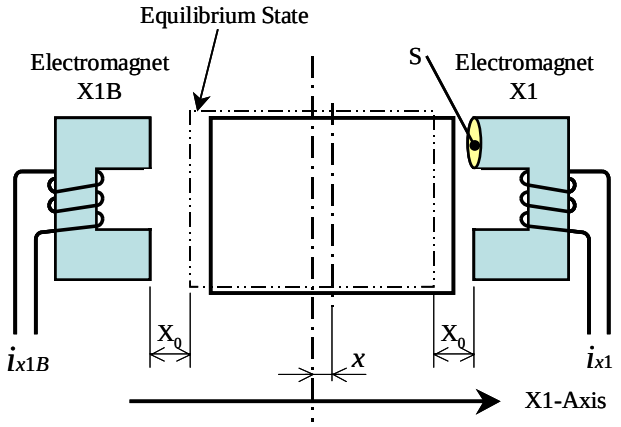

Fig.6 Model of X1-Axis

Fig.7 shows block diagram of feedback system. In addition to zeropower method, the controller composed of the derivative compensator and the notch filter compensate for three bending modes. The integrator is used for generating sufficient static stiffness to cancel the motor negative force.

Fig.8 shows designed transfer function of the AMB controller including the characteristics of anti-aliasing filter, PWM amplifier and coil inductance. To compensate for bending mode of flywheel hub, phase is led up to 650Hz by derivative compensator.

D. Transient Response of Earthquake

Fig.9 is a result of the response analysis of Hanshin-Awaji earthquake which happened in 1995 and caused a severe damage in Japan. The maximum radial displacement of the rotor is about 150 μ m at maximum acceleration of earthquake. In case of Hanshin-Awaji earthquake level, it was confirmed that the rotor would not touch with the touchdown bearing because the gap between these parts is 200 μ m. Hence it is expected that the UPS system would be able to work normally during the earthquake.

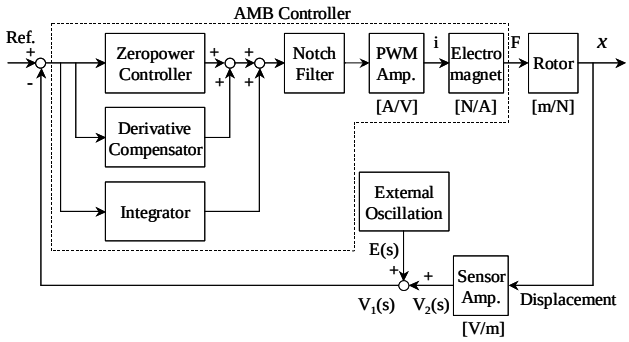

Fig.7 Block Diagram of Feedback System

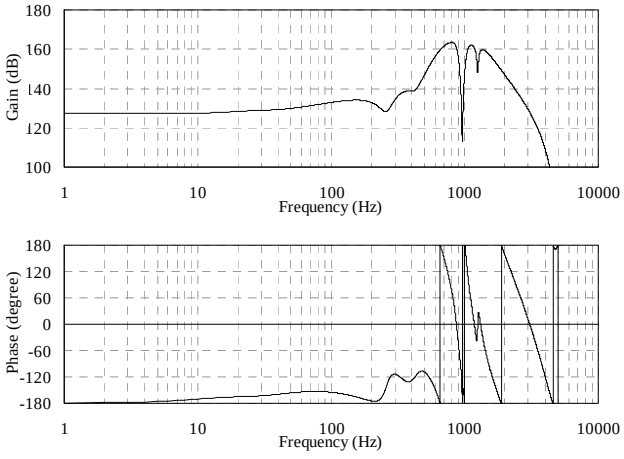

Fig.8 Transfer Function of AMB Controller

IV. Experimental Results

A. Natural Frequency

The AMB could support the rotor up to 13,000min^{-1} at maximum load, 200kW and at no-load with rotating test. Fig.10 shows calculated and measured natural frequencies. The change of the natural frequency of hub bending mode is very large, which is caused by the large gyroscopic effect of flywheel. There is a little difference between calculated and measured ones of 2nd rotor bending mode. Except for its mode, measured ones are similar to calculated ones. Furthermore, measured ones of bending mode of flywheel hub rise about 30Hz over 9,000min^{-1}.

The reason is considered that compression stress between the flywheel hub and the CFRP flywheel varies with rotating speed. In Fig.10, broken line is the result calculated by strengthening stiffness of springs which connect the hub and CFRP flywheel. This calculated result is similar to measured natural frequencies.

Fig.11 shows polar plot on X axes during passing critical speed of two rigid modes. Maximum displacement was about 30 μ m at lower radial AMB. Therefore it was clarified that radial displacement at critical speed had been controlled enough by radial AMBs.

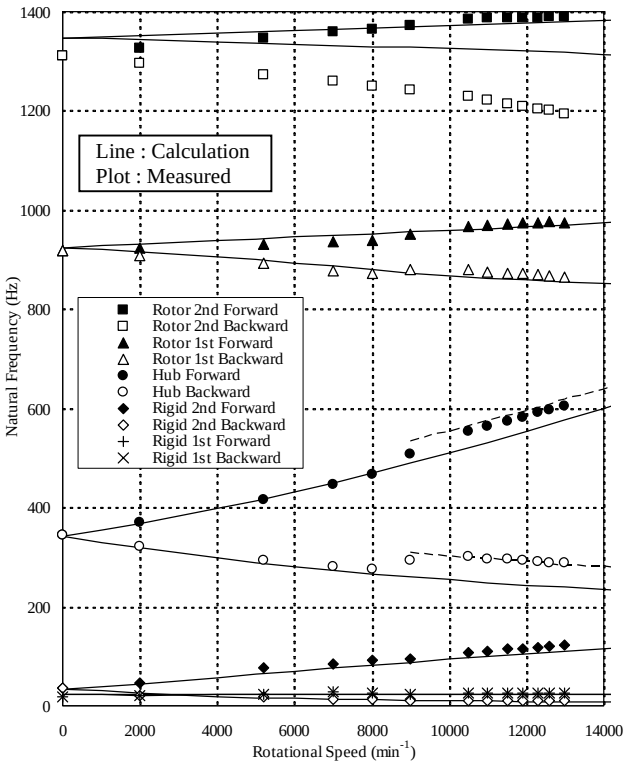

Fig.10 Natural Frequency Map

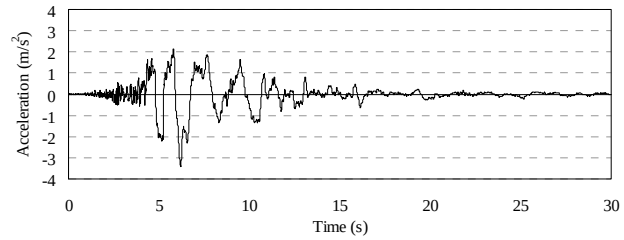

(a) Acceleration Wave of Earthquake

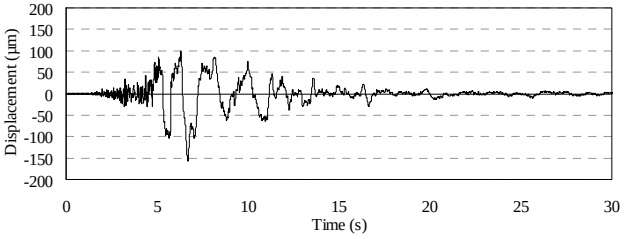

(b) Relative Displacement between Casing and Rotor

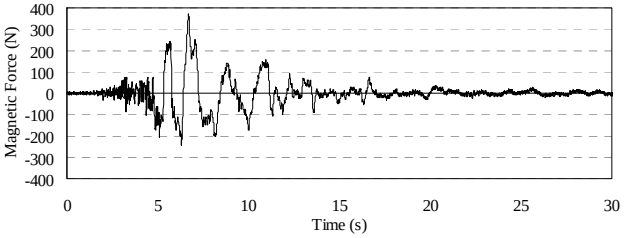

(c) Magnetic Force

Fig.9 Response Analysis of Earthquake

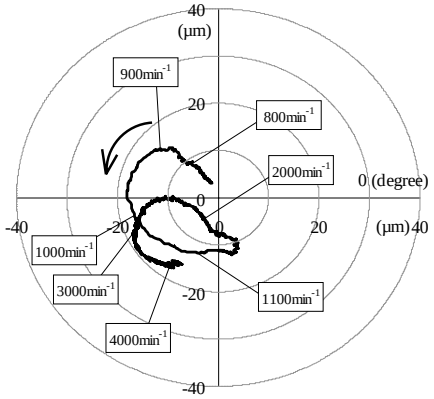

(a) Polar Plot on X1 Axis at Upper Radial AMB

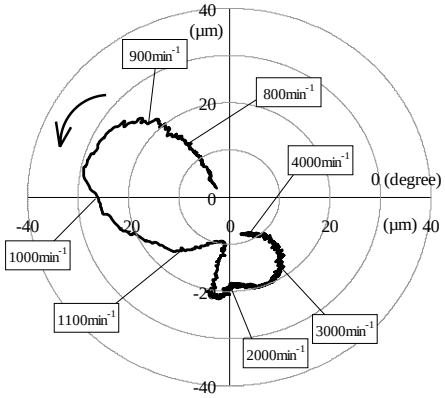

(b) Polar Plot on X2 Axis at Lower Radial AMB

Fig.11 Polar Plot during Passing Rigid Critical Speed

B. *Stability*

The open-loop transfer function $G_o(s)$ and the sensitivity function $G_s(s)$ are expressed as

$$G_o(s) = -V_2(s)/V_1(s) \quad (6)$$

$$G_s(s) = 1/(1+G_0(s)) = V_1(s)/E(s) \quad (7)$$

where $E(s)$ is external oscillation signal, $V_2(s)$ is position sensor output and $V_1(s)$ is the sum of $E(s)$ and $V_2(s)$, and these are shown in Fig.7. $G_s(s)$ is relation to the distance between $G_o(s)$ and the point (-1, 0) on the Nyquist plot. The larger the distance mentioned above is, the smaller $G_s(s)$ is. In short, the system is more stable if Gs(s) is smaller.

In the rotating test, $G_o(s)$ and $G_s(s)$ were measured by sweep excitation up to 1,500Hz. Fig.12 indicates $G_o(s)$ at 0min^{-1} and 13,000min^{-1}. Phase was led up to 640Hz at 0min^{-1}, and it was similar to designed one.

Fig.13 shows $G_s(s)$ at 0min^{-1} and 13,000min^{-1}. For evaluation of the stability margin, zone limit are given by ISO14839-3, therefore this zone limit are applied for this UPS system.

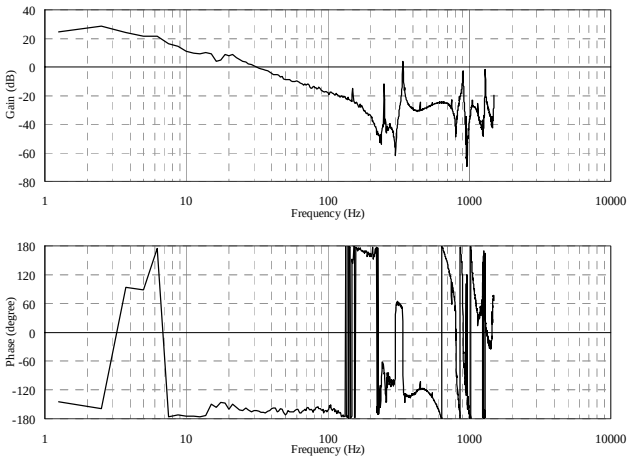

(a) Open-Loop Transfer Function at 0min^{-1}

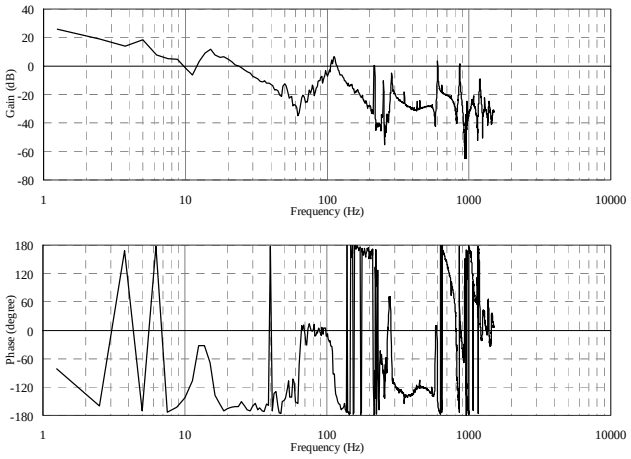

(b) Open-Loop Transfer Function at 13,000min^{-1}

Fig.12 Measured Open-Loop Transfer Function Go(s)

The gain peaks at 0rpm and 13000min^{-1} are all zone A except for only one gain peak. This gain peak of 215Hz at 13,000min^{-1} is zone D. However it is substantially no problem, because 215Hz is a rotating frequency. Hence this system is stable enough.

C. *Coil Current and Mechanical Loss*

Fig.14 shows measured coil current of X1 and X1B. The bias current does not run, and the current controlling unbalance vibration is supplied predominantly. The similar results were obtained about the other axes.

The mechanical loss was measured by the rotational speed drop at free-running. Although mechanical loss includes the AMB loss and the windage loss, the latter is sufficiently small and can be disregarded. The measured mechanical loss is shown in Fig.15. As a result, the AMB loss was very small, about 16W at rated rotational speed.

D. *Continuous Rotating Test*

To measure saturated temperature, continuous rotating test was executed for 10 hours at free-running from rated rotational speed. Fig.16 shows rotational speed and temperature at AMB, the rotor and the motor stator during test.

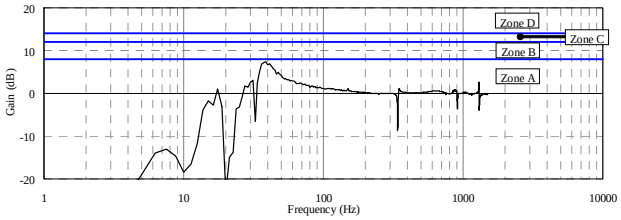

(a) Sensitivity Function at 0min^{-1}

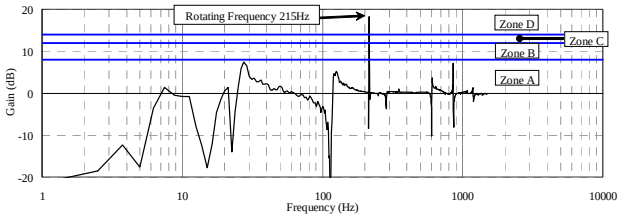

(b) Sensitivity Function at 13,000min^{-1}

Fig.13 Measured Sensitivity Function Gs(s)

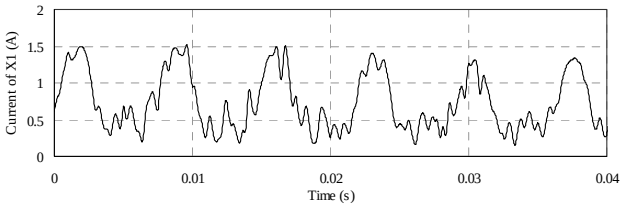

(a) Coil Current of X1

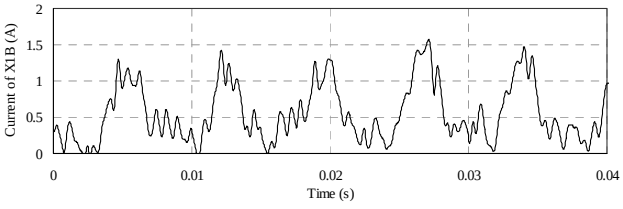

(b) Coil Current of X1B

Fig.14 Measured Coil Current at 9,000min^{-1}

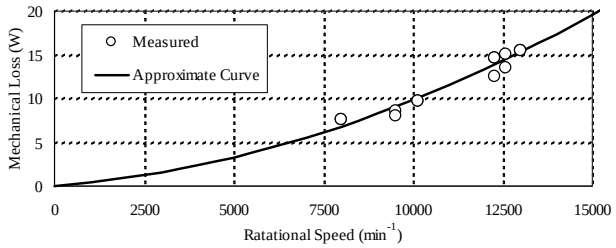

Fig.15 Mechanical Loss

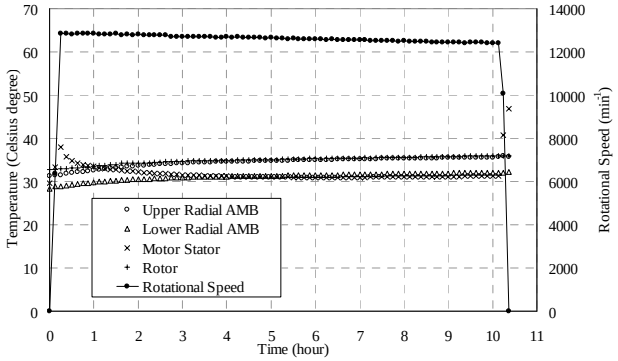

Fig.16 Temperature and Rotational Speed at Continuous Rotating Test

The temperature of AMB and the motor stator was measured by the resistance bulb, and the temperature of the rotor was done by the radiation thermometer. The temperatures almost were saturated, and especially the temperature rise of the rotor was very small, about 4 Celsius degree. In addition, the rotational speed drop was no more than 450min^{-1} for 10 hours, because the mechanical loss was very low. The continuous rotating test is scheduled to execute for much longer time near future.

V. CONCLUSIONS

We designed low loss AMB for the flywheel UPS as follows. The arrangement of the radial AMB was the homo-polar type, and the radial electromagnets were miniaturized and multipolarized in order to decrease the iron loss in the core. The controller for AMB consisted in nonlinear zeropower method, the derivative compensator, the notch filter and the integrator. In response analysis of earthquake, it was confirmed that the rotor would not touch with the touchdown bearing, so it is expected that the UPS system would be able to work normally during the earthquake.

The rotating test shows that AMB could support the rotor up to rated rotational speed at maximum load as well as at no-load, and measured natural frequencies were similar to natural ones calculated.

Stability of the system was evaluated based on ISO14839-3, and it was indicated that the system is stable.

In continuous rotating test, the temperatures rise and the rotational speed drop were small because the mechanical loss was very low.

ACKNOWLEDGMENT

The authors wish to express their gratitude to Dr. Shinobu Saito, Mr. Kenji Matsui, Mr. Ryosei Toyama, Mr. Takashi Majima, Mr. Hisanori Nukumi, Mr. Yuuji Hisa, Mr. Hidefumi Takata, Mr. Kenjirou Yamagishi, Mr. Shunji Kasa and Mr. Kazuaki Kurihara of Ishikawajima-Harima Heavy Industries Co., Ltd. for a lot of helpful advice.

REFERENCES

[1] O. Saito, et. al., Active Magnetic Bearing for 10kW-h Flywheel Energy Storage System, 5th International Symposium on Magnetic Suspension Technology, 1999.

[2] Y.Ariga, K. Nonami, K.Sakai, Nonlinear Control of Zeropower Magnetic Bearing System, Trans. JSME., 67-654, C, 2001.